Visual communications with side information via distributed printing channels: extended multimedia and security perspectives

S.Voloshynovskiy, O. Koval, F. Deguillaume, and T. Pun

University of Geneva - CUI, 24 rue General Dufour, CH 1211, Geneva 4, Switzerland

ABSTRACT

In this paper we address visual communications via printing channels from an information-theoretic point of view as communications with side information. The solution to this problem addresses important aspects of multimedia data processing, security and management, since printed documents are still the most common form of visual information representation. Two practical approaches to side information communications for printed documents are analyzed in the paper. The first approach represents a layered joint source-channel coding for printed documents. This approach is based on a self-embedding concept where information is first encoded assuming a Wyner-Ziv set-up and then embedded into the original data using a Gel'fand-Pinsker construction and taking into account properties of printing channels. The second approach is based on Wyner-Ziv and Berger-Flynn-Gray set-ups and assumes two separated communications channels where an appropriate distributed coding should be elaborated. The first printing channel is considered to be a direct visual channel for images ("analog" channel with degradations). The second "digital channel" with constrained capacity is considered to be an appropriate auxiliary channel. We demonstrate both theoretically and practically how one can benefit from this sort of "distributed paper communications".

Keywords: data-hiding, printed documents, communications with side-information, bar-codes, distributed coding, joint source-channel coding, Gel'fand-Pinsker problem, Wyner-Ziv coding, Berger-Flynn-Gray coding, image enhancement, authentication, integrity control.

1. INTRODUCTION

Printed documents are still the most common, habitual and widely used form of visual information representation. Therefore, as with digital media, the important emerging issues for printed documents are copyright protection, authentication, integrity control, tracking and finally quality enhancement. The printed document can be considered as a part of visual communications where data are converted into some specific form suitable for reliable communications via printing channels, with some given constraints on perceptual quality. Digital halftoning is often used for the transformation of digital documents into printed form. Although, being very simple and having been used since 1855, this transformation unavoidably leads to the degradation of the original document quality. This is not the case for digital documents and has important consequences for document security and management.

Digital data-hiding has been considered as a possible approach to address the above problems for digital documents. However, in most cases the traditional means of digital data-hiding are not always suitable for printed documents and new approaches are required. Moreover, the printing industry has already recognized a limit in the enhancement of printed/scanned image quality related to inverse-halftoning. Further enhancement would imply the development of more expensive and complex printing/scanning devices, which is not appropriate for many low-cost and real-time applications. At the same time the security of printed documents (not necessarily printed on paper) including passports, visas, ID cards, driving licenses, diplomas, credit cards, banknotes or checks is usually accomplished by proprietary know-how technologies and digital data-hiding is far to be widely accepted in this field.

In this paper we consider some practical approaches and analyze several scenarios aiming at further extending the usage of data-hiding technologies for printed documents. This problem is tackled from an information-theoretic point of view as communications with side information. Therefore, the goal of the paper is threefold:

- introduce an information-theoretic formalism into visual communications via distributed printing channels;

- consider possible communications scenarios with side information for multimedia (watermark-assisted) and security applications;

- establish corresponding bounds on system performance assuming side information available at the encoder or at the decoder depending on the particular scenario.

The main practical focus of this paper will be the important problem of quality enhancement of printed documents. Without loss of generality the considered framework can be extended to copyright protection, authentication and tamper proofing applications. Moreover, the proposed framework allows to consider reversible data-hiding from the point of view of multiple access channels and to establish the corresponding rates for the reliable communications of each source, i.e., image and watermark.

To extend the range of possible applications beyond the traditional security documents that represent the major concern of data-hiding and watermarking community as well as security printing industry, we also consider the proposed system on the example of publicly distributed documents such as journals, newspapers, books and advertisement materials. For example, Figure 1 represents the basic system set-up where the image of concern (Lena) should be extracted from the printed document with the purpose of authentication, tracking or quality enhancement. If this image is simply scanned by *a public user* that does not have any access to specific information, the best quality of the resulting scanned image will be defined by the applied processing prior to printing (possibly lossy compression, resampling or blurring), by the quality of the printing and finally by the quality of the scanning (inverse halftoning). It is obvious that in some cases the degradation of quality can be quite considerable so that the scanned image can not be further exploited for the targeted applications.

Moreover, in some practical scenarios, the printed document can not be reproduced in color, if cheap printing is used or when the physics of the reproduction process does not allow to achieve it. One example consists in laser engraving of photos on plastic cards used in security printing. In this case, the color information can be communicated via data-hiding or some auxiliary channel exploiting the redundancy between color planes.
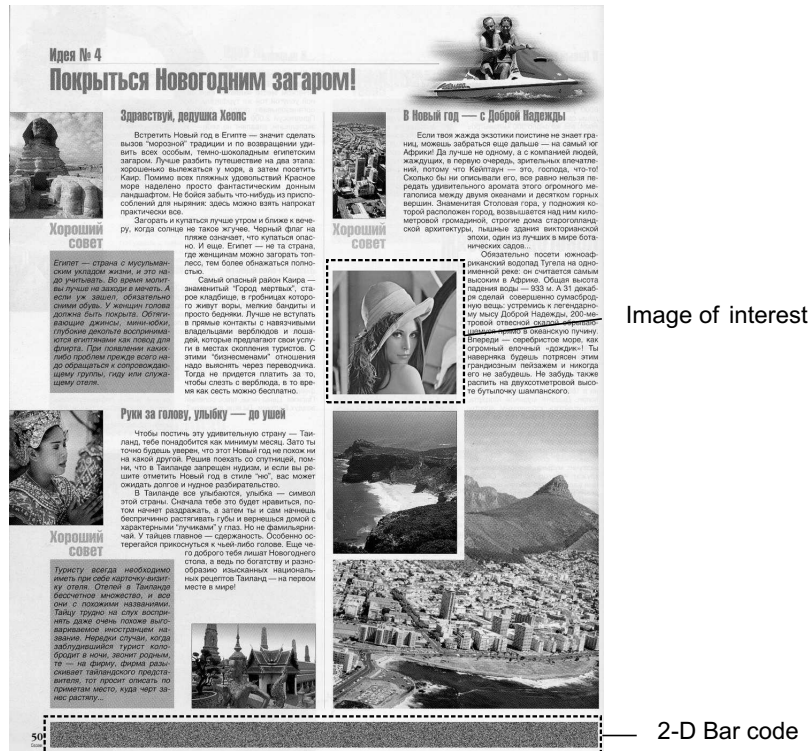

Figure 1. Visual communications via printing channels: example of journal with side information communications.

Another situation arises when the image contains some embedded data or when these data are communicated via some auxiliary channel that can assist the quality enhancement of the printed document. Assume here for simplicity that this auxiliary channel is a 2-D high capacity bar code shown at the bottom of the page (Figure 1) *. The bar code can be designed as a specific pattern or logo to avoid an annoying random-like appearance on the page. The bar code can be also attached on the last page of the journal or on some supplying layout. Access to the embedded data or to the content of the bar code is authorized and can be managed according to the selected distribution protocol. In the simplest case, it can be granted for an extra price. We call the person who has obtained the above access rights *a private user* or *an authorized user*. The private user can somehow benefit from the appropriately communicated extra information in enhancing the quality of the scanned document. Therefore, the overall goal is to design an optimal system that will provide the maximum possible quality of the reconstructed image with minimum needed rate of the extra information to be additionally communicated to the decoder.

In the scope of this paper we propose the further development of digital data-hiding technologies and high capacity bar-codes for printed documents based on communications with side information. We consider two related problems of side information available at the encoder (Gel'fand-Pinsker problem)[1] for host interference cancellation and side information available at the decoder (Wyner-Ziv problem)[2] for distributed coding.

There exist two practical approaches to side information communications for printed documents. The first approach represents a layered joint source-channel coding for printed documents. This approach is based on the self-embedding concept where the information is first encoded assuming Wyner-Ziv set-up and then embedded into the original data using Gel'fand-Pinsker construction and taking into account properties of printing channels.

The second approach is based on the Wyner-Ziv set-up and assumes two separated communications channels where an appropriate distributed coding should be elaborated. The first printing channel is considered to be a direct visual channel for images "analog" channel with degradations). The second "digital channel" with a constrained capacity is considered to be an appropriate bar code. We demonstrate both theoretically and practically how one can benefit from this sort of distributed paper communications using cheap digital printers.

The paper is organized as following. Section 2 outlines the fundamentals of rate-distortion theory with side information. Sections 3 presents a mathematical model of the printing process. Sections 4 and 5 consider possible protocols for self-embedded and auxiliary channel index communications. Section 6 presents experimental results and section 7 concludes the paper.

Notation. We use capital letters to denote scalar random variables X, bold capital letters to denote vector random variables $\mathbf{X}$, corresponding small letters x and $\mathbf{x}$ to denote the realizations of scalar and vector random variables, respectively. The superscript N is used to designate length-N vectors $\mathbf{x} = x^N = [x_1, x_2, ..., x_N]^T$ with ith element x_i. We use $X \sim p_X(x)$ or simply $X \sim p(x)$ to indicate that a random variable X is distributed according to $p_X(x)$. The mathematical expectation of a random variable $X \sim p_X(x)$ is denoted by $E_{p_X}[X]$ or simply by $E[X]$ and $\mathbf{Var}[X]$ denotes the variance of X. Calligraphic fonts $\mathcal{X}$ denote sets $X \in \mathcal{X}$ and $|\mathcal{X}|$ denotes a cardinality of set. $\mathbf{I}_N$ denotes the $N \times N$ identity matrix.

2. VISUAL COMMUNICATIONS WITH SIDE INFORMATION

2.1. Asymmetric two-side information

Visual communications via printing channels can be considered from the point of view of communications with an *asymmetric side information* available at the encoder and at the decoder. The asymmetry of side information originates from the fact that the different types of prior information are available at the encoder before the printing process, and actual side information available a posteriori at the decoder. Let S_1 denotes the side information available at the encoder and S_2 the side information available at the decoder (Figure 2). One can consider S_1 as a "virtually predicted" image after halftoning/inverse halftoning and S_2 as the physically printed and scanned image. Assume that $\{X_k, S_{1,k}, S_{2,k}\}$ are i.i.d. $\sim p_{X,S_1,S_2}(x, s_1, s_2)$ independent drawings of jointly distributed random variables $X \in \mathcal{X}$, $S_1 \in \mathcal{S}_1$ and $S_2 \in \mathcal{S}_2$ where $\mathcal{X}, \mathcal{S}_1, \mathcal{S}_2$ are finite sets. A distortion measure is defined as $d(x, \hat{x})$ and the corresponding average distortion as $D = \frac{1}{N} \sum_{k=1}^{N} E[d(X_k, \hat{X}_k)]$. The sequence $\{X_k\}$ is encoded in blocks of length N into a binary stream of rate R, which should be decoded back as a sequence $\{\hat{X}_k\}$ in the reproduction alphabet.

---

*Note: more generally auxiliary channel can be designed using different information carriers used in the printed (plastic) documents such as bar codes, invisible inks or crystals, magnetic strips, cheap electronic low-capacity chips.
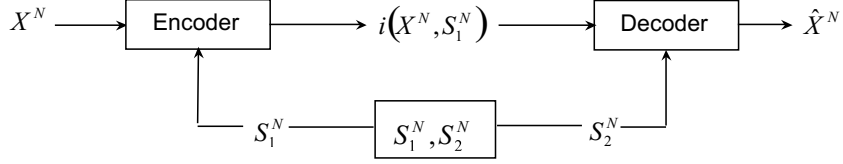
Figure 2. Two-sided asymmetric side information available at both encoder and decoder.

Cover and Chiang[3] have shown that the rate R is achievable at the distortion level D, if there exists a sequence of $(2^{NR}, N)$ codes $i : \mathcal{X}^N \times \mathcal{S}_1^N \to \{1, 2, \cdots, 2^{NR}\}$, $\hat{X} : \{1, 2, \cdots, 2^{NR}\} \times \mathcal{S}_2^N \to \hat{\mathcal{X}}^N$ such that $E[d(X^N, \hat{X}(i(X^N, S_1^N), S_2^N))] = D$:

$$R(D) = \min_{p(u|x,s_1)p(\hat{x}|u,s_2)} [I(U; S_1, X) - I(U; S_2)], \tag{1}$$

where the minimization is under the distortion constraint $\sum_{x,u,s_1,s_2,\hat{x}} d(x, \hat{x})p(x, s_1, s_2)p(u|x, s_1)p(\hat{x}|u, s_2)) \leq D$ and U is an auxiliary random variable. $S_2 \to (X, S_1) \to U$ and $(X, S_1) \to (U, S_2) \to \hat{X}$ form Markov chains.

2.2. Symmetric two-side information

To introduce the basic concept of visual communications via printing channels for the broad set of different application scenarios considered in the following sections, we will simplify the previous set-up to a symmetric side information $S = S_1 = S_2$ that can be available at both encoder and decoder or only at the decoder according to Figure 3.
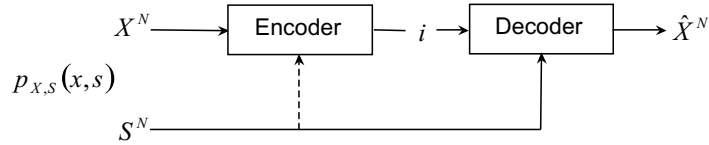

Figure 3. Symmetric side information $S_1 = S_2 = S$.

2.2.1. Symmetric side information at both encoder and decoder

The rate-distortion with symmetric side information at both encoder and decoder $S = S_1 = S_2$ was considered by Berger[4] and Flynn-Gray[5] (Figure 3: dashed line corresponds to availability of S^N at the encoder). A code $(2^{NR}, N)$ consists of an encoding map $i : \mathcal{X}^N \times \mathcal{S}^N \to \{1, 2, \cdots, 2^{NR}\}$ and a reconstruction map $\hat{X} : \{1, 2, \cdots, 2^{NR}\} \times \mathcal{S}^N \to \hat{\mathcal{X}}^N$. Therefore, both encoder $i(.)$ and decoder $\hat{X}(.)$ depend on the state S^N. The corresponding rate-distortion function is defined as:

$$R_{X|S}(D) = \min_{p(\hat{x}|x,s)} I(X; \hat{X}|S), \tag{2}$$

where the minimization is over all $p(\hat{x}|x, s)$ such that $\sum_{x,\hat{x},s} d(x, \hat{x})p(x, s)p(\hat{x}|x, s) \leq D$. The above rate-distortion-function also follows from (2) assuming $S = S_1 = S_2$.[3]

2.2.2. Side information at decoder

The rate-distortion problem with side information available at the decoder was considered by Wyner and Ziv.[2] It also follows from (1), if $S_1 = \emptyset$, $S_2 = S$ and $(S_1, X) = X$:

$$R(D)_{X|S}^{WZ} = \min_{p(u|x)p(\hat{x}|u,s)} [I(U; X) - I(U; S)] = \min_{p(u|x)p(\hat{x}|u,s)} I(U; X|S), \tag{3}$$

where the minimization is performed over all $p(u|x)p(\hat{x}|u, s)$, i.e., $p(x, s, u, \hat{x}) = p(x, s)p(u|x)p(\hat{x}|u, s)$ for fixed $p(x, s)$, and all decoder functions $\hat{X}(i(X), S)$ such that $\sum_{x,\hat{x},u,s} p(x, s) p(u|x)p(\hat{x}|u, s)d(x, \hat{x}) \leq D$ and $|\mathcal{U}| \leq |\mathcal{X}| + 1$. The

second equality in (3) follows from the fact that $S \rightarrow X \rightarrow U$ form a Markov chain (note: the second Markov chain is formed as $X \rightarrow (U; S) \rightarrow \hat{X}$).

The random coding strategy in the Wyner-Ziv (W-Z) set-up is as follows: given the distribution $p_{U|X}(u|x)$ and the encoding function $i(.)$, generate $2^{NI(U;X)}$ i.i.d. sequences U^N according to $\prod_{k=1}^{N} p_U(u_k)$ and distribute them randomly into $2^{N(I(U;X)-I(U;S))}$ bins. Given the source sequence $\mathbf{x}$, the encoder looks for a unique $\widetilde{\mathbf{u}}$ such that it is jointly typical with $\mathbf{x}$. The source is compressed to the index of the bin i that contains the $\widetilde{\mathbf{u}}$. Given side information $\mathbf{s}$ and index $i \in \{1, 2, \cdots, 2^{N(I(U;X)-I(U;S))}\}$ the decoder looks in bin i for a sequence $\mathbf{u}$ which is jointly typical with $\mathbf{s}$ and generates the reproduction sequence $\hat{\mathbf{x}}(\mathbf{u}, \mathbf{s})$. In the general case, $I(\hat{X}; X|S) \leq I(U; X|S)$ and therefore it can be a *loss* in performance of the Wyner-Ziv set-up in comparison to the rate-distortion function with side information available at both encoder and decoder.

We will denote the classic rate-distortion function without any side information ($S_1 = \emptyset$, $S_2 = \emptyset$) as:

$$R(D) = \min_{p(\hat{x}|x)} I(\hat{X}; X), \tag{4}$$

where the minimization is performed over all $p(\hat{x}|x)$ such that $\sum_{x,\hat{x}} p(x)p(\hat{x}|x)d(x, \hat{x}) \leq D$.

2.2.3. Shannon lower bound (SLB): Gaussian source and MSE distortion

No side information: The classic rate-distortion function without any side information for a Gaussian $\mathcal{N}(0, \sigma_X^2)$ source with squared error distortion is represented by the SLB[6]:

$$R(D) = \frac{1}{2} \log_2^+ \frac{\sigma_X^2}{D}, \tag{5}$$

where $\log_2^+ x = \max\{0, x\}$. The corresponding rate-distortion function simultaneously describing N independent Gaussian random variables (*a parallel Gaussian source model*) $X_k \sim \mathcal{N}(0, \sigma_{X_k}^2)$, $k = 1, 2, \cdots, N$ with a rate R bits/source vector is given by:

$$R(D) = \sum_{k=1}^{N} \frac{1}{2} \log_2 \frac{\sigma_{X_k}^2}{D_k}, \tag{6}$$

where

$$D_k = \begin{cases} \lambda, & \text{if } \lambda < \sigma_{X_k}^2, \\ \sigma_{X_k}^2, & \text{if } \lambda \geq \sigma_{X_k}^2, \end{cases} \tag{7}$$

where λ is chosen to satisfy $\sum_{i=1}^{N} D_k = D$.

Side information at encoder and decoder: Let $\mathbf{X} = X^N = \{X_1, X_2, \cdots, X_N\}$ be zero mean and stationary Gaussian memoryless source $\mathbf{X} \sim \mathcal{N}(\mathbf{0}, \sigma_X^2 \mathbf{I}_N)$. The side information is given by a noisy version of source $\mathbf{S} = \mathbf{X} + \mathbf{Z}'$ where $\mathbf{X}$ and $\mathbf{Z}'$ are independent and $\mathbf{Z}' \sim \mathcal{N}(\mathbf{0}, \sigma_{Z'}^2 \mathbf{I}_N)$, and the vector joint PDF is $p_{\mathbf{X},\mathbf{S}}(\mathbf{x}, \mathbf{s}) = \prod_{k=1}^{N} p_{X_k, S_k}(x_k, s_k)$. The joint PDF for each pair (X_k, S_k) can be represented as:

$$p_{X_k, S_k}(x_k, s_k) = p_{S_k}(s_k) p_{X_k|S_k}(x_k|s_k) = \frac{1}{\sqrt{2\pi\sigma_S^2}} e^{-\frac{s_k^2}{2\sigma_S^2}} \frac{1}{\sqrt{2\sigma_{X|S}^2}} e^{-\frac{\left(x_k - \rho \frac{\sigma_X}{\sigma_S} s_k\right)^2}{2\sigma_{X|S}^2}}, \tag{8}$$

where $\sigma_{X|S}^2 = \sigma_X^2(1 - \rho^2)$ is conditional variance.

Define a sample-wise covariance matrix $\mathbf{C}_{XS}$ between all N pairs of (X_k, S_k):

$$\mathbf{C}_{XS} = \begin{bmatrix} \mathbf{Var}[X] & \mathbf{Cov}[X, S] \\ \mathbf{Cov}[S, X] & \mathbf{Var}[S] \end{bmatrix} = \begin{bmatrix} \sigma_X^2 & \rho\sigma_X\sigma_S \\ \rho\sigma_X\sigma_S & \sigma_S^2 \end{bmatrix}, \tag{9}$$

where $|\rho| < 1$ for all k and $\sigma_S^2 = \sigma_X^2 + \sigma_{Z'}^2$. $\mathbf{Cov}[X, S] = E[X(X + Z')] = \sigma_X^2$ and $\rho = \frac{\mathbf{Cov}[X,S]}{\sqrt{\mathbf{Var}[X]\mathbf{Var}[S]}} = \frac{\sigma_X}{\sigma_S}$.

If the encoder observes $\mathbf{S}$, then the encoder and the decoder can each compute a minimum mean squared error (MMSE) estimate of $\mathbf{X}$ as a conditional mean:

$$\hat{\mathbf{X}}' = E[\mathbf{X}|\mathbf{S}]. \tag{10}$$

In this case, it is sufficient to communicate only the difference:

$$\mathbf{Z} = \hat{\mathbf{X}}' - \mathbf{X}, \tag{11}$$

with the defined average distortion D. If we define $\rho^2 = \frac{\sigma_X^2}{\sigma_S^2}$, we can express the variance of the estimation as $\sigma_{X|S}^2 = (1 - \rho^2)\sigma_X^2 = \frac{\sigma_X^2 \sigma_{Z'}^2}{\sigma_X^2 + \sigma_{Z'}^2}$ and $\mathbf{Z} \sim \mathcal{N}(\mathbf{0}, \sigma_{X|S}^2 \mathbf{I}_N)$. Therefore, the rate-distortion function will have the same character as for the stationary Gaussian source:

$$R(D)_{X|S} = \frac{1}{2} \log_2^+ \frac{\sigma_{X|S}^2}{D}. \tag{12}$$

Consequently, the rate saving due to the available side information at the encoder and the decoder with respect to the independent coding of X is:

$$R(D) - R(D)_{X|S} = \frac{1}{2} \log_2 \frac{1}{1 - \rho^2}. \tag{13}$$

If $\rho^2 \to 0$, i.e., the variance of the noise Z' is increasing and X and S become less correlated, $R(D)_{X|S} \to R(D)$ and no gain can be expected from the joint decoding.

In the case of non-stationary Gaussian vector (parallel Gaussian source), we have similarly to (6):

$$R(D)_{X|S} = \sum_{k=1}^{N} \frac{1}{2} \log_2 \frac{\sigma_{X_k}^2 \sigma_Z^2}{(\sigma_{X_k}^2 + \sigma_Z^2)D_k}, \tag{14}$$

where

$$D_k = \begin{cases} \lambda, \text{ if } \lambda < \frac{\sigma_{X_k}^2 \sigma_Z^2}{\sigma_{X_k}^2 + \sigma_Z^2}, \\ \frac{\sigma_{X_k}^2 \sigma_Z^2}{\sigma_{X_k}^2 + \sigma_Z^2}, \text{ if } \frac{\sigma_{X_k}^2 \sigma_Z^2}{\sigma_{X_k}^2 + \sigma_Z^2}, \end{cases} \tag{15}$$

where λ is chosen to satisfy $\sum_{i=1}^{N} D_k = D$.

Side information at decoder: Wyner and Ziv[2,7] demonstrated that for the Gaussian case $R(D)_{X|S}^{WZ} = R(D)_{X|S}$. However, the equality does not hold for the case of any PDF of source $\mathbf{X}$. Therefore, generally $R(D)_{X|S}^{WZ} \geq R(D)_{X|S}$. This means that there is a rate loss with Wyner-Ziv coding. Also it is known that for discrete sources when $D = 0$, the Wyner-Ziv problem reduces to the Slepian-Wolf problem[8] with $R(0)_{X|S}^{WZ} = R(0)_{X|S} = H(X|S)$ assuming that S is communicated to the decoder at the rate $H(S)$.

Approaching theoretical rate-distortion function with symmetric side-information (Wyner-Ziv vs Berger-Flynn-Gray set-ups): For practical reasons, we will perform a comparative analysis of the non-collaborative encoding set-up (Wyner-Ziv problem) with collaborative one (Berger-Flynn-Gray problem) for distributed coding in printing applications.

In the general case, the following "inequality sandwich" is valid:

$$R(D) \geq R(D)_{X|S}^{WZ} \geq R(D)_{X|S}. \tag{16}$$

Therefore, the rate-distortion function $R(D)_{X|S}^{WZ}$ for the non-collaborative encoders is above the rate-distortion function $R(D)_{X|S}$ for the collaborative encoders. In our particular case of distributed coding with side information in printing applications, the side information at the encoder is naturally given by the physical nature of the problem. That is not the case in e.g. the distributed coding of correlated sources in remote sensing applications where no collaboration is assumed between the encoders due to their space/time displacement. Therefore, the printing application should definitively benefit from the availability of side information at the encoder. Moreover, there are three main additional factors that impact the performance of Wyner-Ziv distributed coding, i.e., PDF of the source, dimensionality/complexity of practical implementation and performance in low SNR-regime.

PDF of the source X: It is desirable to have the equality $R(D)_{X|S}^{WZ} = R(D)_{X|S}$ for any source distribution. However, this equality holds only for the Gaussian PDF. Zamir[9] also shown that in the case of any source PDF and MSE distortion measure, the difference between two rate-distortion functions can be bounded by 1/2 bit:

$$R(D)_{X|S}^{WZ} - R(D)_{X|S} \leq \frac{1}{2}, bit. \tag{17}$$

However, it should be noted that this bound is not tight. Therefore, contrarily to the channel coding with side information available at the encoder, where the channel capacity is shown to be invariant to the noise PDF[10,11] (this argument should be used with care with respect to the scenario and corresponding operational regime), the investigation of "dual" problem in distributed coding of correlated sources with side information at the encoder remains an open challenging problem.

Dimensionality/complexity: In most practical situations we are interested in simple and tractable solutions leading to efficient coding strategies. The already established approach due Zamir *et al*[12] and Pradhan and Ramchandran[13] is to consider the Wyner-Ziv problem based on *lattices* and *cosets*.

We introduce an N-dimensional *lattice* Λ as a discrete additive subgroup of real N-space $\mathbb{R}^N$.[14] A volume $V(\Lambda)$ per lattice point (or the volume of the Voronoi region) $\mathcal{V}(\Lambda)$ is defined as:

$$V(\Lambda) = \int_{\mathcal{V}(\Lambda)} d\mathbf{x}, \tag{18}$$

where $\mathcal{V}(\Lambda) = \{\mathbf{x} \in \mathbb{R}^N : \|\mathbf{x}\|^2 = \min_{\mathbf{c} \in \Lambda} \|\mathbf{x} - \mathbf{c}\|^2\}$ is the Voronoi region and $\mathbf{c}$ is a lattice point.

The Shannon lower bound (SLB) for the source $\mathbf{X} \in \mathbb{R}^N$ and any N-dimensional quantizer and MSE distortion measure is:

$$R(D) \geq h(\mathbf{X}) - \frac{N}{2} \log_2 \left(\frac{2\pi e D}{N} \right). \tag{19}$$

The SLB becomes tight in the limit as D goes to zero:

$$R(D) = h(\mathbf{X}) - \frac{N}{2} \log_2 \left(\frac{2\pi e D}{N} \right). \tag{20}$$

To characterize a lattice, one often refers to the *normalized second moment* $G(\Lambda)$ (or dimensionless second moment) of a region $\mathcal{V}(\Lambda)$:

$$G(\Lambda^N) = \frac{1}{N V(\Lambda)^{1+2/N}} \int_{\mathcal{V}(\Lambda)} \|\mathbf{x}\|^2 \, d\mathbf{x}. \tag{21}$$

The normalized second moment of any version of the integer lattice $\mathbb{Z}$ (including $\mathbb{Z}^2$ or even $\mathbb{Z}^N$, for any N) is $G(\mathbb{Z}) = 1/12$. It is also know that the normalized second moment of the N-sphere is $G(\Lambda^N) = 1/2\pi e$ as $N \to \infty$.

Practical lattice quantizers working in the high-rate regime (density of the source X is assumed to be smooth within a quantization bin) and MSE distortion always have rate loss (redundancy) and are above the SLB. For example, the entropy of a scalar quantizer for the source $X \in \mathbb{R}^1$ in the high-rate regime (or small distortion regime):

$$H(Q_1(X)) = h(X) - \frac{1}{2} \log_2(12D). \tag{22}$$

The entropy of any N-dimensional lattice quantizer that encodes a "smooth" source $\mathbf{X} \in \mathbb{R}^N$ is:

$$H(Q_N(X)) = h(\mathbf{X}) - \frac{N}{2} \log_2 \left(\frac{D}{N G(\Lambda^N)} \right). \tag{23}$$

Therefore, the asymptotic rate redundancy of an entropy coded lattice quantizer (23) above the SLB (20) is $\frac{1}{2} \log_2 \left(2\pi e G(\Lambda^N) \right)$. If one chooses a "good" lattice such as $G(\Lambda^N) \to 1/2\pi e$, it is possible to reduce this redundancy to zero. However, in many practical situations of uniform quantizers (with $\mathbb{Z}$ lattice) this redundancy can be as large as $\pi e/6$ (1.53 dB). Even using a hexagonal lattice A_2 which has $G(A_2) = 5/(36\sqrt{3})$, one still has redundancy $\frac{1}{2} \log_2 \left(10\pi e/(36\sqrt{3}) \right)$ (1.37 dB).

Therefore, the existence of "good" source codes occurs in asymptotically high-dimensional spaces. This leads to high-dimensional systems that might not be always suitable for many practical applications. It should also be noticed that most of state-of-the-art classical coders without side information are based on simple content-adaptive scalar quantizers, i.e., even not an 2-D (vector) quantizers besides their obvious advantages. Therefore, one often sacrifices performance for the sake of a simple and efficient implementation. This practical constraint can also act as the bounding factor of rate loss in distributed coding.

Low-SNR regime: It is known in the dual problem of channel coding with side information that lattice-based schemes (including QIM and SCS,[15] inflated lattices[11]) have considerable loss in performance due to boundary lattice effect in low watermark-to-noise ratio (WNR) regime (contrarily to the bounded shaping loss at high WNR-regime). Since the Wyner-Ziv problem exploits the same design rules for noisy side information, the boundary effect of corresponding channel code part can manifest itself in a loss of performance. Therefore, when $\rho^2 \to 0$, one should use a "powerful" channel code. However, at the same time (this will be shown later in Figure 11), a possible gain due to the side information presence with respect to the classic coding vanishes, and one can only expect a significant enhancement for reliable side information, i.e., when $\rho^2 \to 1$. Therefore, contrarily to the remote sensing applications of distributed source coding, where the side information can be considerably distorted leading to small values of ρ^2, in printing applications one should benefit from the fact that the user has overall control on the printing process and that the availability of side information at the encoder should lead to simple and efficient solutions.

2.2.4. Compressed channel index communication

In printed documents, the side information S^N is directly available as the printed image (possibly after inverse halftoning). However, the index i should be somehow communicated to the decoder in practical systems. There exist two possible solutions:

- communicate index i via the printed image itself using "self-embedding" (data-hiding);

- communicate index i via *auxiliary channel* that can include different information carriers used in the printed (plastic) documents such as bar codes, invisible inks or crystals, magnetic strips, cheap electronic low-capacity chips.

3. MATHEMATICAL MODEL OF PRINTING

To investigate the "quality" of side information, i.e., to establish how close S is correlated with X from one side and to investigate the possibility of self-embedded communications from another side, one should consider a mathematical model of a printing channel.

3.1. Halftoning and inverse halftoning: image processing perspectives

Digital halftoning is a process that converts a gray-scale image ($X \in \{0, 1, \cdots, 255\}$) into a bi-level image ($X \in \{0, 255\}$) that can easily be reproduced by a simple printing device. There are two types of haltoning, i.e., ordered and random (or so-called error diffusion) halftoning. The ordered halftoning is mostly used in laser printers while error diffusion represents a broad class of ink jet printing devices. We will focus on the later for demonstration purposes. The error diffusion takes the error from the quantized gray-scale pixel to bi-level pixel and diffuses the quantization error over a causal neighborhood. The inverse halftoning of error diffusion should ensure that the spatially-localized average pixels values of the halftone and original gray-scale image are similar. Kite *et al*[16] proposed an accurate linear model for error diffusion halftoning. This model accurately predicts the "blue noise" (high-frequency noise) and edge sharpening effects observed in various error-diffused halftones. The resulting halftone image $\mathbf{s}$ is obtained as:

$$\mathbf{s} = H\mathbf{x} + Q\mathbf{w} = H\mathbf{x} + \mathbf{z}', \tag{24}$$

where H represents a linear shift-invariant (LTI) halftone filter, Q is a LTI filter corresponding to the error diffusion coloring, $\mathbf{w}$ is white noise and $\mathbf{z}' = Q\mathbf{w}$ is colored noise.

Therefore, the *inverse halftoning* according to (24) can be posed as a deconvolution or restoration problem (in image processing) or channel equalization problem (in digital communications) where operator H represents the equivalent blurring or channel and $\mathbf{z}'$ corresponds to the image acquisition or channel noise.

The distributed coding system with communications via printing channels is shown in Figure 4. The physical printing channel is represented as a sequential set of operations comprising halftoning, printing and scanning. Here, we assume that printing itself, as the black point reproduction process with a specified resolution, and scanning do not introduce any distortions. In more general case one would need to take into account some optical blurring and aberrations as well as sensor non-linearity.
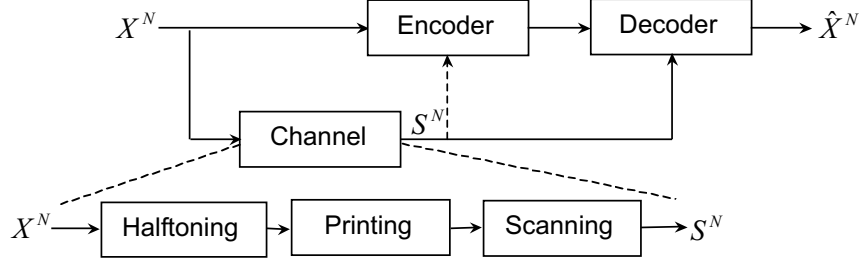
Figure 4. Printing channel communication setup.

Considering the halftoning problem according to the vector channel (24), one can assume without loss of generality vector Gaussian signals $\mathbf{X} \sim \mathcal{N}(\mathbf{0}, \mathbf{C}_X)$ and $\mathbf{Z}' \sim \mathcal{N}(\mathbf{0}, \mathbf{C}_{Z'})$. In this case, the deconvolution problem can be formulated as the MMSE estimation of $\mathbf{x}$ given by the the conditional mean $\hat{\mathbf{X}}' = E[\mathbf{X}|\mathbf{S}]$:

$$\hat{\mathbf{x}}' = \left(H^T \mathbf{C}_{Z'}^{-1} H + \mathbf{C}_X^{-1}\right)^{-1} H^T \mathbf{C}_{Z'}^{-1} \mathbf{s} = H_W \mathbf{s}, \tag{25}$$

where $H_W = \left(H^T \mathbf{C}_{Z'}^{-1} H + \mathbf{C}_X^{-1}\right)^{-1} H^T \mathbf{C}_{Z'}^{-1}$ represents a Wiener "restoration/equalization" filter.

The estimation error $\mathbf{Z} = \hat{\mathbf{X}}' - \mathbf{X} = E[\mathbf{X}|\mathbf{S}] - \mathbf{X}$ is also Gaussian $\mathbf{Z} \sim \mathcal{N}(\mathbf{0}, \mathbf{C}_Z)$ due to linear nature of the MMSE estimate where the covariance matrix is defined as:

$$\mathbf{C}_Z = \mathbf{C}_{X|S} = E[(\hat{\mathbf{x}}' - \mathbf{x})(\hat{\mathbf{x}}' - \mathbf{x})^T] = \left(H^T \mathbf{C}_{Z'}^{-1} H + \mathbf{C}_X^{-1}\right)^{-1}. \tag{26}$$

The halftoning/inverse haftoning printing channel can be sequentially represented by an equivalent channel shown in Figure 5.
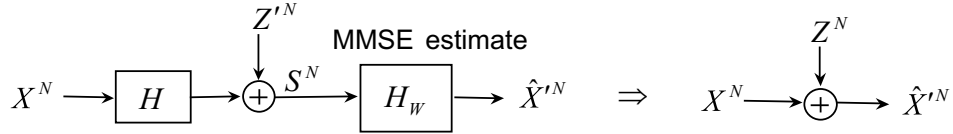

Figure 5. Equivalent halftoning/inverse halftoning channel.

3.2. Equivalent channel: information-theoretic perspectives

The goal of this section is to extend the results obtained for the channel equialization problem to the inverse halftoning and to show that the inverse halftoning is information lossless. Cioffi *et al*[17] proved for a similar problem of channel equalization that the MMSE estimation is information lossless showing that:

$$I(\mathbf{X}; \mathbf{S}) = I(\mathbf{X}; \hat{\mathbf{X}}'). \tag{27}$$

This follows from the fact that the MMSE estimate is linear and the estimation error $\mathbf{Z}$ is independent of $\hat{\mathbf{X}}'$. In particular, it was shown that[17]:

$$I(\mathbf{X}; \mathbf{S}) = h(\mathbf{S}) - h(\mathbf{S}|\mathbf{X}) = \frac{1}{2} \log_2 \frac{\det |\mathbf{C}_S|}{\det |\mathbf{C}_{S|X}|} = \frac{1}{2} \log_2 \frac{\det |\mathbf{C}_S|}{\det |\mathbf{C}_{Z'}|} = \frac{1}{2} \log_2 \frac{\det |H^T \mathbf{C}_X H + \mathbf{C}_{Z'}|}{\det |\mathbf{C}_{Z'}|}, \tag{28}$$

$$I(\mathbf{S}; \mathbf{X}) = h(\mathbf{X}) - h(\mathbf{X}|\mathbf{S}) = \frac{1}{2} \log_2 \frac{\det |\mathbf{C}_X|}{\det |\mathbf{C}_{X|S}|} = \frac{1}{2} \log_2 \frac{\det |\mathbf{C}_X|}{\det |\mathbf{C}_Z|} = \frac{1}{2} \log_2 \frac{\det |\mathbf{C}_X|}{\det |\left(H^T \mathbf{C}_{Z'}^{-1} H + \mathbf{C}_X^{-1}\right)^{-1}|}, \tag{29}$$

where det $|.|$ denotes the determinant and $\mathbf{C}_{S|X} = \mathbf{C}_{Z'}$ and $\mathbf{C}_{X|S} = \mathbf{C}_Z$. Since $I(\mathbf{X}; \mathbf{S}) = I(\mathbf{S}; \mathbf{X})$, it follows that $\frac{1}{2} \log_2 \frac{\det |\mathbf{C}_S|}{\det |\mathbf{C}_{Z'}|} = \frac{1}{2} \log_2 \frac{\det |\mathbf{C}_X|}{\det |\mathbf{C}_Z|}$.

3.3. Inverse halftoning: practical low-complexity algorithm

In this section we will extend the results obtained for i.i.d. Gaussian signals to real images. The key issue is the availability of an accurate, simple and tractable stochastic image model leading to a close form solution. Although stochastic inverse halftoning is a stand-alone important problem, we will use here the state-of-the-art inverse halftoning method proposed by Neelamani *et al*[18] for wavelet-based inverse halftoning via deconvolution (WInHD). This approach is based on the original idea of Donoho[19] called *wavelet-vaguelette decomposition*. The wavelet-vaguelette decomposition splits the deconvolution problem into two parts. In the first part, the operator H in (24) is inverted leading to the "deblurred" estimate:

$$\widetilde{\mathbf{x}} = H^{-1}\mathbf{s} = \mathbf{x} + H^{-1}Q\mathbf{z}', \tag{30}$$

that produces the clean image $\mathbf{x}$ with noisy part $H^{-1}Q\mathbf{z}'$ assuming that the inverse operator H^{-1} exists (that it is not the case in general for all image restoration problem).

The second part of wavelet-vaguelette decomposition tries to remove the noisy part $H^{-1}Q\mathbf{z}'$ using wavelet-based denoising. Therefore, the relevant problem of stochastic image modeling is reduced to the proper modeling of wavelet coefficients. A. Hjorungnes, J. Lervik and T. Ramstad[20] have proposed a simple and tractable model that has found a number of applications in state-of-the-art image coding (EQ-coder[21]), denoising (wavelet Wiener filter[22]) and watermarking for evaluation of data-hiding capacity[23] and content-adaptive data-hiding.[24] According to the EQ framework, image coefficients are considered coming from a realization of independent Gaussian distribution with a "slowly" varying variance. This represents a class of local Gaussian models and justifies the application of local operations. It should be mentioned that the relationship between the global image statistics and locally Gaussian assumption was elegantly demonstrated based on mixture model where the variance also becomes a random parameter drawn from the exponential distribution.[20] This also justifies a doubly stochastic modeling of image coefficients and provides a logical connection to the parallel Gaussian source model considered in section 2.2.3.

The denoiser of WInHD is also based on the same model that leads to the Wiener filter as the MMSE (MAP) estimate for Gaussian case. To enhance the performance of the denoiser, the WInHD implements the Wiener filter in an overcomplete transform domain (complex wavelets) to overcome the problems of the critically sampled wavelet transform. Thus the final estimate is obtained as:

$$\hat{x}'_{j,k} = \frac{\sigma^2_{j,k}}{\sigma^2_{j,k} + \sigma^2_j}\widetilde{x}_{j,k}, \tag{31}$$

where j denotes the scale, $\sigma^2_{j,k}$ the local variance of image coefficients for scale j, σ^2_j the variance of the residual noisy term in the transform domain and all variables are considered in the transform domain.

It is not our primary goal to enhance the WInHD, we will use it in its original form. It should however be mentioned that more powerful stochastic image models could be used, taking into account the stationarity of transform image coefficients along the edges and transitions. Such models should bring additional enhancement of the inverse halftone image quality and corresponding higher reliability of side information at the decoder.[25]

4. INDEX COMMUNICATION VIA SELF-EMBEDDING

4.1. Index communication via self-embedding: gray-scale image embedding

According to the set-up represented in Figure 3 the index of the codeword in the compressed channel should be available to the decoder. It can be directly communicated via the image itself. This kind of communications has many common features with the digital upgrade of analog transmissions proposed by Puri *et al*[26] and the layered joint source-channel coding considered by Barron *et al*[27] and Merhav and Shamai.[28]

Digital data-hiding can be used for index communication via self-embedding. In this case, the host data X is available at the encoder non-causally, i.e., the whole vector can be used for the design of the optimal codebook. Therefore, this scheme can be considered as communications with side information available at the encoder. This problem can be formulated as a reliable communication of message i, encoded into a codeword W, over the channel with noise Z and interference X being known at the encoder but not at the decoder. The corresponding discrete memoryless channel is described by $\{\mathcal{W}, p_{S|W,X}(s|w,x), \mathcal{S}, \mathcal{X}\}$ where the side information has distribution $p_X(x)$ (Figure 6). Given an auxiliary random variable U with conditional distribution $p_{U|X}(u|x)$ and a deterministic

encoding function $h : \mathcal{U}^N \times \mathcal{X}^N \to \mathcal{W}^N$ such that $S \to (W, X) \to U$ forms a Markov chain, Gel'fand and Pinsker[1] have shown using a random binning argument that the capacity of this channel is[1]:

$$C = \max_{p(u,w|x)} \left[I(U; S) - I(U; X) \right]. \tag{32}$$

It should be pointed that the host image X and the watermark W are independent in this set-up. Given side information $\mathbf{x}$ and message $i \in \{1, 2, ..., 2^{N(I(U;S)-I(U;X))}\}$ the encoder looks in bin i for a sequence $\mathbf{u}$ which is jointly typical with $\mathbf{x}$ and transmits $\mathbf{w} = h(\mathbf{u}, \mathbf{x})$. The decoder receives $\mathbf{s}$ and looks for a unique $\widetilde{\mathbf{u}}$ sequence that is jointly typical with $\mathbf{s}$. The index of the bin which contains the $\widetilde{\mathbf{u}}$ is decoded as the message $\widehat{i}$.
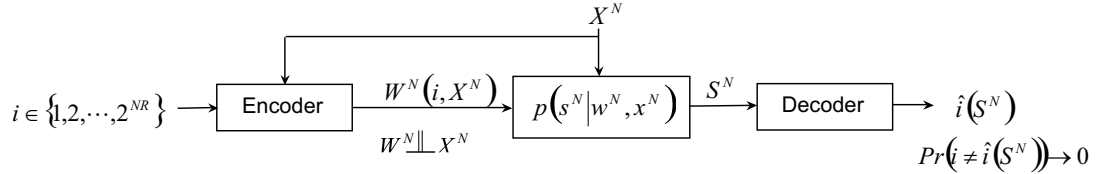

Figure 6. Gel'fand-Pinsker channel coding with side information at the encoder.

Costa considered the above problem in a Gaussian context and found that:

$$C = \frac{1}{2} \log_2 \left(1 + \frac{\sigma_W^2}{\sigma_Z^2} \right), \tag{33}$$

where the auxiliary random variable has a form of $U = W + \alpha X$ and $\alpha = \frac{\sigma_W^2}{\sigma_W^2 + \sigma_Z^2}$ is chosen to provide independence of $W - \alpha(W + Z)$ and $W + Z$. This means that the capacity with the interference signal available at the encoder and AWGN channel is the same as the capacity of a simple AWGN channel without interference.

The source coding with side information can be performed based on the Wyner-Ziv problem considered in section 2. Puri *et al*[26] proposed a practical implementation of the Wyner-Ziv problem using cosets.

Combining the source coding with the channel coding we obtain the joint layered system shown in Figure 7.
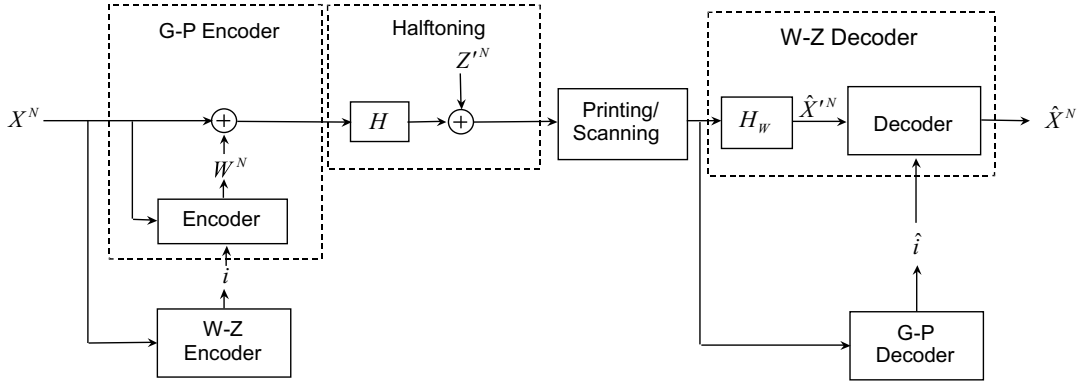

Figure 7. Layered source-channel coding system with index communication via self-embedding in gray-scale image.

The proposed joint source-channel coding can work in two different regimes assuming two main types of users, i.e., public users and private users. The public users can have direct access only to the printed image and the maximum quality that can be obtained in this case is determined by the MMSE estimation:

$$\hat{\mathbf{x}}^{pub} = \left(H^T (H^T \mathbf{C}_W H + \mathbf{C}_{Z'})^{-1} H + \mathbf{C}_X^{-1} \right)^{-1} H^T (H^T \mathbf{C}_W H + \mathbf{C}_{Z'})^{-1} \mathbf{s}, \tag{34}$$

that produces the overall estimation error:

$$D_{MMSE}^{pub} = trace[\mathbf{C}_{X|S}^{pub}] \tag{35}$$

with the estimation error covariance matrix equal to:

$$\mathbf{C}_{X|S}^{pub} = \left(H^T(H^T\mathbf{C}_W H + \mathbf{C}_{Z'})^{-1}H + \mathbf{C}_X^{-1}\right)^{-1}. \tag{36}$$

In the private decoding case, the authorized users will additionally have access to the hidden (communicated) information communicated with the rate R. This facilitates a possibility to perform the MMSE estimation and Wyner-Ziv decoding that should result in superior image quality:

$$D^{priv} = trace[\mathbf{C}_{X|S}^{pub}]2^{-2R}. \tag{37}$$

In the case of Costa communications with $R = C$ and previous Gaussian set-up one obtains:

$$D^{priv} = trace[\mathbf{C}_{X|S}^{pub}]\frac{\det|\mathbf{C}_{Z'}|}{\det|H^T\mathbf{C}_W H + \mathbf{C}_{Z'}|}. \tag{38}$$

Therefore, it is obvious that one can expect the enhanced quality private communications with the factor of 2^{-2R} over public communications. However, it should be noted that the scheme we discuss here assumes complete independence between the watermark and the host image. It is interesting to compare the performance of the above layered system with uncoded analog transmissions considered by Gallager[29] where the "watermark" can be designed to be collinear to the host that is addressed in our ongoing research.

4.2. Index communication via self-embedding: gray-scale image embedding using joint precoding and Gel'fand-Pinsker encoding

In the previous set-up the halftoning channel leads to intersymbol interference due to the filter H. Obviously, one can benefit from the knowledge of the operator H at the encoder using *precoding* at the encoder. The precoding was originally proposed by Tomlinson and Harashima[30–32] for band-limited channels. The Tomlinson-Harashima precoding (T-HP) has a lot in common with the G-P problem and can also be designed using modulo-M operation or quantizer taking into account the known relationship $w \mod M = w - Q(w)$, where $Q(w)$ is the corresponding quantizer and $w \mod w$ represents a quantization error. One can also consider a multidimensional lattice version of the modulo operation (mod Λ) with respect to the vector $\mathbf{w}$: $\mathbf{w} \mod \Lambda = \mathbf{w} - Q(\mathbf{w})$. In the case of $\mathbb{Z}$ lattices, there is also a 1.53 dB loss from capacity due to the shaping. More advanced schemes combining coding, precoding and shaping are analyzed by Eyuboglu and Forney[33] and Fischer *et al.*[32] The block-diagram of joint precoding and Gel'fand-Pinsker encoding is shown in Figure 8. This scheme is working similarly to the previous set-up with the only difference that the knowledge of the host image is used at the Gel'fand-Pinsker encoding while the T-HP is exploiting knowledge of the filter H. In the extended version, it is possible to formulate a joint problem of host and intersymbol interference cancellation, i.e., instead of double sequential projection one can design a joint lattice to avoid a double requantization, the analysis of which is going beyond the scope of this paper.

4.3. Index communication via self-embedding: bi-level image embedding

Another possibility exists to cancel intersymbol interference in the case when the user has the complete control over the printing process. In this case, the index can be directly embedded into the halftone image (bi-level) image. The block-diagram explaining this embedding is shown in Figure 9. In this case, watermark embedding is performed after filter H and the watermark extraction is accomplished before inverse halftoning.

The problem of joint halftoning-data-hiding can be specifically formulated for error-diffusion halftoning. Notably, this possibility was considered by Fu and Au[34] where a sufficient payload was reported to be generated for halftone image embedding.
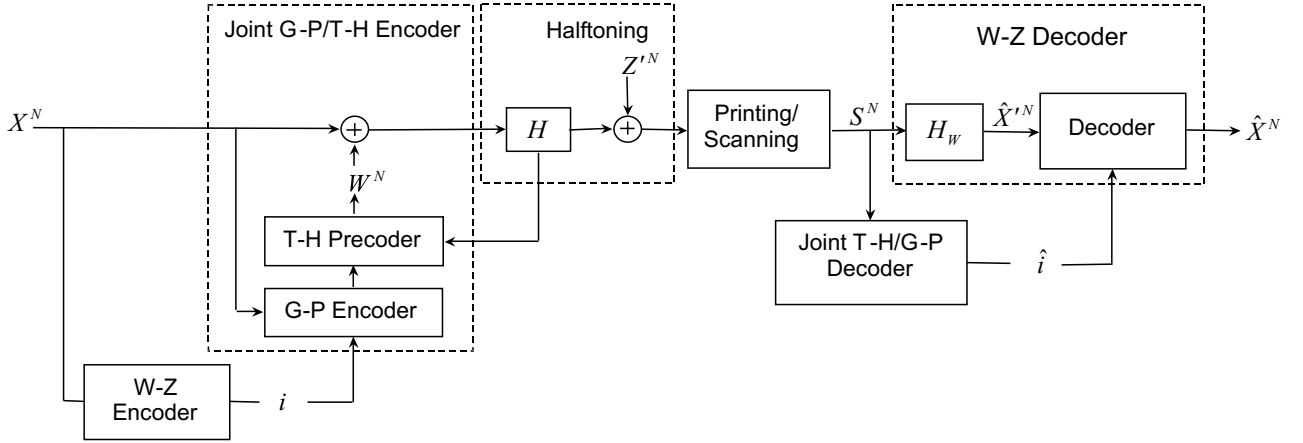
Figure 8. Layered source-channel coding system with index communication via self-embedding in gray-scale image and T-HP.
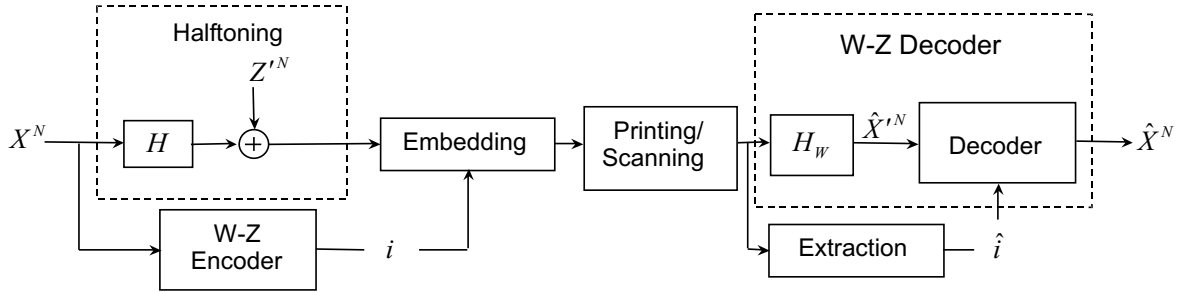

Figure 9. Layered source-channel coding system with index communication via self-embedding in bi-level image.

5. INDEX COMMUNICATION VIA AUXILIARY PHYSICAL CHANNEL

The approach based on the index communication via auxiliary physical channel can be designed either using the Berger-Flynn-Gray set-up, i.e., symmetric two-sided information, or the Wyner-Ziv set-up, i.e., side information available only at the decoder. The basic system block-diagram for both set-ups is shown in Figure 10 with the difference consisting in the availability of side information S^N at the encoder.

Contrarily to the system with index communication via self-embedding, the auxiliary physical channel index communications have several advantages. First, since the index is communicated via the "external" auxiliary channel and no data-hiding is required, the host (analog) image has no extra distortions due to the watermark embedding. It is an important argument for preservation of printed image quality as well as for the availability of more reliable side information S at the decoder. Secondly, the capacity of the auxiliary channel is only determined by the possible printing area and printing/scanning resolution contrarily to the self-embedding system where capacity is constrained by the ratio $\frac{\sigma_W^2}{\sigma_Z^2}$, i.e., by the allowed distortions in the printed image. The difference between these capacities can be significant for different practical applications and should be carefully analyzed for each particular case. Therefore, we will consider the performance of the two-sided Berger-Flynn-Gray set-up as a *lower bound* for source coding with side information.

The practical design of the auxiliary channel index communication system includes two main functional blocks, namely source coding for the residual compression and channel coding (2-D bar code) for index communication.

Source coding: To establish the lower bound for the rate-distortion function we will consider here only the Berger-Flynn-Gray set-up assuming that the Wyner-Ziv system will do the best to approach this bound using multidimensional lattice/coset codes. According to the analysis presented in sections 2.2.3 and 3, we assume that the side information which is given in the form of analog (halftone) image is also available at the encoder due
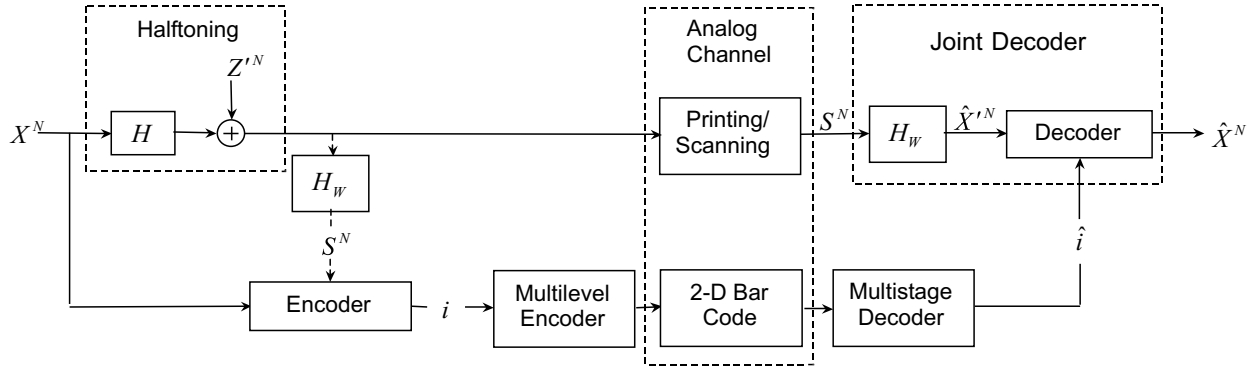
Figure 10. Index communication via auxiliary (2-D bar code) channel.

to the complete knowledge of the printing process. Thus, the encoder should only communicate the difference $\mathbf{Z} = E[\mathbf{X}|\mathbf{S}] - \mathbf{X}$ to the decoder with the given bounded distortion D choosing corresponding index $i(\mathbf{X}, \mathbf{S})$. Therefore, for the stationary Gaussian source and the MSE distortion measure the rate-distortion function of this scheme will be defined by the equation (12).

Channel coding: The task of the channel code in the above scheme is to communicate errorlessly ($Pr(i \neq \hat{i}(S^N)) \rightarrow 0$) the index i via some analog auxiliary channel. A natural auxiliary channel for printed documents consists of 2-D bar codes,[35] although as was mentioned in the introduction other types of information carriers with sufficient capacity can be used for this purpose. In the case of 2-D bar codes, *multilevel codes* (MLC)[36,37] can be used for errorless index communication. The MLC are known to closely approach capacity for band-limited channels. The main idea of multilevel coding consists in the protection of each address bit of the signal point by an individual binary code $\mathcal{C}^\ell$ at level ℓ. One can use irregular low-density parity-check (LDPC) codes as the binary code $\mathcal{C}^\ell$ for each level ℓ followed by 8-PAM chosen for simplicity reasons and easy integration into printed 2-D bar code. One can also apply precoding for bar-codes to avoid intersymbol interference caused by the halftoning filter H. Finally, *multistage decoding* is applied based on multiple access channel decomposition of MLC using chain rule for mutual information between channel output and each level. Due to the space restriction of this paper we will not consider all details concerning the practical construction of 2-D bar-code, that might also include more involved schemes including bit interleaved MLC.

6. RESULTS

First, to investigate the theoretical limits of source coding with side information available at both encoder and decoder, we have modeled the rate-distortion function $R(D)_{X|S}$ for a Gaussian source and the MSE distortion measure for different values of ρ^2 (Figure 11). The highest gain with respect to the classic coding without side information can be expected for highly correlated sources X and S (reliable side information) when $\rho^2 \rightarrow 1$. If $\rho^2 \rightarrow 0$, there is no gain with respect to $R(D)$. Therefore, the printing channel (and particularly a joint halftoning/inverse halftoning) should provide an accurate estimate of the source X, i.e., to reduce the impact of the halftoning process. In real applications, ρ^2 is expected to be in the range of $0.2 \leq \rho^2 \leq 0.6$ and therefore for the stationary Gaussian source the maximum gain can be as much as 0.26-0.66 bit per sample.

Secondly, we have performed the comparison of different coding strategies for a number of real images based on Floyd halftoning and wavelet-based inverse haftoning via deconvolution.[18] Here we only report results for the image Lena of size of 512×512. The "*lower empirical bound*" is estimated for the Berger-Flynn-Gray set-up described in section 5. The prediction of the inverse halftone image **s** based on the MMSE estimate ($\hat{\mathbf{X}}' = E[\mathbf{X}|\mathbf{S}]$) is performed at the encoder and the residual $\mathbf{Z} = \hat{\mathbf{X}}' - \mathbf{X}$ is compressed at various rates and communicated to the decoder via 2-D bar code. At the decoder, the MMSE estimate **S** is computed from the printed image and combined with the decoded residual $Q(\mathbf{Z})$.

Three different lossy coders are used to compress the residual $Q(\mathbf{Z})$, i.e., the DCT-based JPEG, wavelet-based WaveConvert[38] and wavelet-based EQ coder (4 level DWT based on 9/7 pair with local variance ML estimate in a causal window of size 3×3 without interscale dependencies)[21] for rates 0.20, 0.25, 0.50 and 1.00 bpp. The results of

modeling for rate 0.20 bpp are shown in Figure 12. For comparison reasons, we also indicate in Table 1 the results of direct compression by the above methods assuming that one can directly communicate the compressed image via 2-D bar code to the decoder without usage of side information for final image reconstruction. A possible gain due to the decoding with the side information in the form of a halftone image is also shown in the table. The PSNR of the inverse halftone image (with respect to the original image) was 31.95 dB after WInHD for all tests. The maximum gain is obtained for the EQ coder, and is in the range of 0.26-2.50 dB for different rates with respect to the directly compressed image. Obviously, the capacity of the auxiliary channel will be a factor that determines a particular operational rate depending on the application constraints. The enhancement of "analog" (halftone) image quality is also varying for different rates between 3-8 dB, which indicates a considerable potential of such an "upgrade" for many practical applications where the image quality should be relatively high. Using advanced methods of inverse halftoning and more accurate stochastic image models one can expect a further enhancement of image quality for low-bit rates.
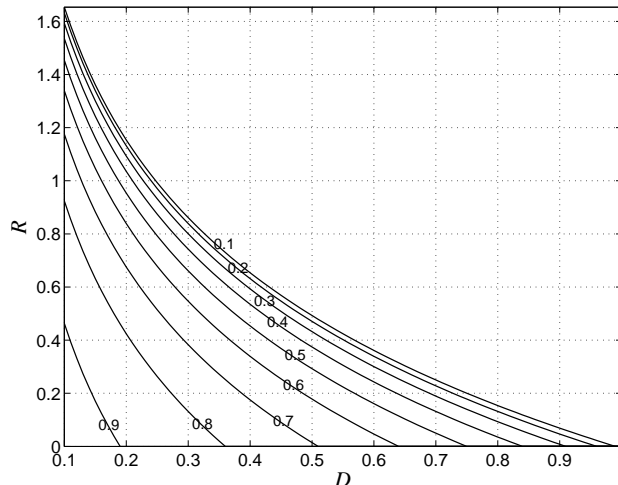

Figure 11. Conditional rate-distortion function for different ρ and $X \sim \mathcal{N}(0, 1)$.

7. CONCLUSIONS

We have considered the problem of visual communications with side information via distributed printing channels. Besides "classical" applications of digital data-hiding technologies such as copyright protection and authentication, we have considered the possibility of watermark- or side information-assisted image processing in printing applications. In particular the problem of image quality enhancement was considered. We have also provided a mathematical modeling of the printing channel in the scope of digital communications with side information. The related problems of source coding based on Wyner-Ziv and Berger-Flynn-Gray set-ups and channel coding based on Gel'fand-Pinsker problem have been considered. Corresponding practical scenarios have been analyzed and finally the theoretical bounds on systems performance are given. The results of computer simulation show a range of possible applications where the expected gain can considerably increase the possibilities and functionalities of modern multimedia and security systems.
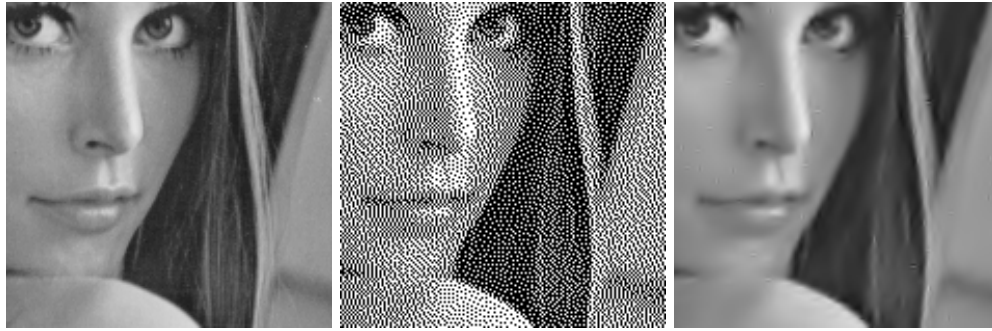
Table 1. Comparison of resulting PSNR [dB] for several compression methods.

Compression method	Rate [bpp]			
	0.20	0.25	0.50	1.00
DCT-based JPEG coder				
Direct compression	28.89	30.41	34.64	37.83
Compression with SI	33.55	34.17	36.19	38.61
Gain over direct compression	**4.66**	**3.76**	**1.55**	**0.78**
Gain over direct halftoning WInHD	**1.60**	**2.22**	**4.24**	**6.66**
WaveConvert coder				
Direct compression	32.47	33.48	36.59	39.66
Compression with SI	35.11	35.39	37.77	40.03
Gain over direct compression	**2.64**	**1.91**	**1.18**	**0.37**
Gain over direct halftoning WInHD	**3.16**	**3.44**	**5.82**	**8.08**
EQ-based coder				
Direct compression	32.87	34.11	37.20	40.40
Compression with SI	35.42	35.90	38.24	40.76
Gain over direct compression	**2.55**	**1.79**	**1.04**	**0.36**
Gain over direct halftoning WInHD	**3.47**	**3.95**	**6.29**	**8.81**

REFERENCES

1. S. Gel'fand and M. Pinsker, "Coding for channel with random parameters," *Problems of Control and Information Theory* **9**(1), pp. 19–31, 1980.
2. A. Wyner and J. Ziv, "The rate-distortion function for source coding with side information at the decoder," *IEEE Trans. Information Theory* **22**, pp. 1–10, January 1976.
3. T. Cover and M. Chiang, "Duality of channel capacity and rate distortion with two sided state information," *IEEE Trans. on Information Theory* **48**(6), 2002.
4. T. Berger, *The information theory approach to communications (G. Longo ed.), chapter Multiterminal Source Coding*, Springer-Verlag, 1978.
5. T. J. Flynn and R. M. Gray, "Encoding of correlated observations," *IEEE Trans. Information Theory* **33**, pp. 773–787, Nov 1987.
6. T. Cover and J. Thomas, *Elements of Information Theory*, Wiley and Sons, New York, 1991.
7. A. Wyner, "The rate-distortion function for source coding with side information at the decoder-II: General sources," *Information and Control* **38**, pp. 60–80, 1978.
8. D. Slepian and J. Wolf, "Noiseless encoding of correlated information sourcea," *IEEE Trans. Information Theory* **19**, pp. 471–480, July 1973.
9. R. Zamir, "The rate loss in the wyner-ziv problem," *IEEE Trans. Information Theory* **19**, pp. 2073–2084, November 1996.
10. A. Cohen and A. Lapidoth, "Generalized writing on dirty paper," in *International Symposium on Information Theory (ISIT)*, (Lausanne, Switzerland), July 2002.
11. U. Erez, S. Shamai, and R. Zamir, "Capacity and lattice-strategies for cancelling known interference," in *Proc. of ISITA 2000*, pp. 681–684, (Honolulu, Hawaii), November 2000.
12. R. Zamir, S. Shamai, and U. Erez, "Nested linear/lattice codes for structured multiterminal binning," *IEEE Trans. Information Theory* **48**, pp. 1250–1276, June 2002.
13. S. Pradhan and K. Ramchandran, "Distributed source coding using syndromes (DISCUS): design and construction," *IEEE Trans. on Information Theory* **49**, pp. 626–643, March 2003.
14. G. D. Forney, M. D. Trott, and S. Chung, "Sphere-bound-achieving coset codes and mutilevel codes," *IEEE Trans. on Information Theory* **46**, pp. 820–850, May 2000.

Figure 12. Results of computer modeling for the frame of Lena image: (a) original image Lena; (b) halftone image; (c) WInHD inverse halftone image; (d) directly JPEG compressed image (rate 0.2 bpp); (e) JPEG compressed image with side information (rate 0.2 bpp); (f) directly EQ compressed image (rate 0.2 bpp); (g) EQ compressed image with side information (rate 0.2 bpp).

15. J. Eggers, J. Su, and B. Girod, "A blind watermarking scheme based on structured codebooks," in *Secure images and image authentication, IEE Colloquium*, pp. 4/1–4/6, (London, UK), April 2000.

16. T. Kite, B. Evans, A. Bovik, and T. Sculley, "Modeling and quality assessment of halftoning by error diffusion," *IEEE Trans. Image Processing* **9**, pp. 909–922, May 2000.

17. J. Cioffi, G. Dudevoir, M. Eyuboglu, and D. J. Forney, "MMSE decision-feedback equalizers and coding: Part I: Equalization results and part II: Coding results," *IEEE Trans. Communications* **43**, pp. 2582–2582, Oct 1995.

18. R. Neelamani, R. Nowak, and R. G. Baraniuk, "WInHD: Wavelet-based inverse halftoning via deconvolution," *submitted to IEEE Trans. Image Processing* , Oct 2002.

19. D. Donoho, "Nonlinear solution of linear inverse problems by wavelet-vaguelette decomposition," *Applied and Computational Harmonic Analysis* **2**, pp. 101–126, 1995.

20. A. Hjorungnes, J. Lervik, and T. Ramstad, "Entropy coding of composite sources modeled by infinite gaussian mixture distributions," in *IEEE Digital Signal Processing Workshop*, pp. 235–238, 20-24 January 1996.

21. S. LoPresto, K. Ramchandran, and M. Orhard, "Image coding based on mixture modeling of wavelet coefficients and a fast estimation-quantization framework," in *Data Compression Conference 97*, pp. 221–230, (Snowbird, Utah, USA), 1997.

22. M. K. Mihcak, I. Kozintsev, K. Ramchandran, and P. Moulin, "Low-complexity image denoising based on statistical modeling of wavelet coefficients," *IEEE Signal Processing Letters* **6**, pp. 300–303, December 1999.

23. P. Moulin and M. K. Mihcak, "A framework for evaluating the data-hiding capacity of image sources," *IEEE Trans. on Image Processing* **11**, pp. 1029–1042, September 2002.

24. S. Voloshynovskiy, A. Herrigel, N. Baumgaertner, and T. Pun, "A stochastic approach to content adaptive digital image watermarking," in *Third International Workshop on Information Hiding*, vol. 1768, pp. 212–236, (Dresden, Germany), September 29 - October 1st 1999.

25. S. Voloshynovskiy, O. Koval, and T. Pun, "Wavelet-based image denoising using non-stationary stochastic geometrical image priors," in *IS&T/SPIE's Annual Symposium, Electronic Imaging 2003: Image and Video Communications and Processing V*, (Santa Clara, California USA), 20-24 January 2003.

26. R. Puri, K. Ramchandran, and S. S. Pradhan, "On seamless digital upgrade of analog transmission systems using coding with side information," in *Allerton Conf. Communication, Control, and Computing*, (Allerton, IL, USA), October 2002.

27. R. Barron, B. Chen, and G. Wornell, "The duality between information embedding and source coding with side information and some applications," *IEEE Trans. Information Theory* **49**, pp. 1159–1180, May 2003.

28. N. Merhav and S. S. (Shitz), "On joint source-channel coding for the wyner-ziv source and the gel'fand-pinsker channel," *IEEE Trans. Information Theory* , to appear 2003.

29. R. Gallager, *Information theory and reliable Communication*, J. Wiley and Sons, 1968.

30. T. Tomlinson, "New automatic equalizer employing modulo arithmetic," *Electronics Letters.* , pp. 138–139, March 1971.

31. H. Harashima and H. Miyakawa, "Matched-transmission technique for channels with intersymbol interference," *IEEE Trans. on Communications* , pp. 774–780, August 1972.

32. R. Fischer, W. Gerstacker, and J. Huber, "Dynamics limited precoding, shaping, and blind equalization for fast digital transmission over twisted pair lines," *IEEE Journal on Selected Areas in Communications (JSAC), (Special Issue: Advanced Techniques for Digital Transmission via Copper Lines)* **13**, pp. 1622–1633, December 1995.

33. M. V. Eyuboglu and G. D. Forney, "Trellis precoding: Combined coding, precoding and shaping for intersymbol interference channels," *IEEE Trans. on Information Theory* **38**, pp. 301–314, March 1992.

34. M. Fu and O. Au, "Data hiding in halftone images using stochastic error diffusion," in *Proceedings IEEE Int. Conf. On Acoustics, Speech and Signal Processing*, vol. 3, pp. 1965–1968, (Salt Lake City, Utah, USA), May 2001.

35. N. Degara-Quintela and F. Perez-Gonzalez, "Visible encryption: Using paper as a secure channel," in *Security and Watermarking of Multimedia Contents V*, vol. 5020, (Santa Clara, California USA), 20-24 January 2003.

36. H. Imai and S. Hirakawa, "A new multilevel coding method using error-correcting codes," *IEEE Trans. on Information Theory* **3**, pp. 371–377, May 1995.

37. J. Huber, U. Wachsmann, and R. Fischer, "Coded modulation by multilevelcodes: Overview and state of the art," in *ITG–Fachbericht: Codierung fur Quelle, Kanal und Ubertragung*, pp. 255–266, (Aachen, Germany), March 1998.

38. T. Strutz, "Waveconvert, http://www-nt.e-technik.uni-rostock.de/ $\sim$ ts/software/download.html," 2001.